Dissociation of polycyclic aromatic hydrocarbons at high energy: MD/DFTB simulations versus collision experiments

Aude Simon, Jean-Philippe Champeaux, Mathias Rapacioli, Patrick Moretto-Capelle, Florent X. Gadéa, Martine Sence

Noname manuscript No.
(will be inserted by the editor)

Dissociation of polycyclic aromatic hydrocarbons at high energy : MD/DFTB simulations vs collision experiments.

Fragmentation paths, energy distribution and internal conversion : test on the pyrene cation.

A. Simon* · J. P. Champeaux · M. Rapacioli · P. Moretto Capelle · F. X Gadéa · M. Sence

Received: date / Accepted: date

Abstract The whole process following collisions of polycyclic aromatic hydrocarbons (PAHs) with high energetic protons is modeled and compared to the experimental mass spectrum, allowing to propose a coherent scenario. Fragmentation of cationic pyrene $C_{16}H_{10}^{+}$ is extensively studied by molecular dynamics simulations obtained by computing the electronic structure at the Self-Consistent-Charge Density Functional based Tight Binding (MD/SCC-DFTB) on-the-fly. An atomic model is used to quantify the energy transfered to the target after proton impact, and assuming fast internal conversion for the produced cations. From this model, after ionisation, the molecules show a broad distribution of internal energy with a rough exponential decrease. This distribution is used as an input for further extensive MD/SCC-DFTB simulations. The good agreement between experimental and theoretical spectra globally validates the SCC-DFTB potential, the wide distribution of fragments corresponding to statistical dissociation. The scenario for both the internal energy deposited distribution and the fast internal conversion assumption is validated. Using these assumptions, dissociation is shown to occur within a few hundreds of picoseconds. Moreover, adjusting the experimental mass spectrum with the theoretical spectra obtained for the various internal energies nicely returns the distribution modeled from the atomic contributions, reinforcing the coherence of the global approach. This study lays the foundations for further synergistic theoretical and experimental studies that will be devoted to other PAHs and prebiotic molecules of astrophysical interest.

Keywords DFTB · molecular dynamics · energy internal conversion · polycyclic aromatic hydrocarbons · dissociation · high energy collisions

A. Simon*, M. Rapacioli and F. X. Gadéa
Lab. Chim. & Phys. Quant. LCPQ/IRSAMC, UMR5626 Université de Toulouse & CNRS, UT3-Paul Sabatier, 118 Route Narbonne, F-31062 Toulouse, France.
*Corresponding author, Tel: +33 (0)5 61 25 88 73; E-mail: aude.simon@irsamc.ups-tlse.fr
J. P. Champeaux, P. Moretto Capelle and M. Sence
Lab. Coll. Atom. & React. LCAR/IRSAMC, UMR5589 Université de Toulouse & CNRS, UT3-Paul Sabatier, 118 Route Narbonne, F-31062 Toulouse, France.

1 Introduction

Polycyclic Aromatic Hydrocarbons (PAHs) are organic compounds composed of multiple aromatic carbonaceous rings edged by hydrogen atoms. Interest for PAHs in the astrophysical community arose in the mid-eighties as a PAH population was proposed as the carrier of the Aromatic Infrared Bands (AIBs) [24,1], a set of mid-IR emission bands [18] ubiquitous in the InterStellar Medium (ISM). However, despite a longstanding synergy between astronomical observations and laboratory investigations, no specific PAH molecule has yet been identified [21]. In fact, one of the reasons for the identification problem may come from the competition between IR emission, isomerisation and dissociation (see ref. [12] for instance). More generally, the investigation of energetic processing of astroPAHs is currently an important research topic as it can significantly impact the physics and chemistry of the ISM [44]. In this respect, efforts are currently made, both experimentally and theoretically, to probe the possible relationship between astro-PAHs and recently observed simple aromatic potential precursors such as benzonitrile[28], or carbonaceous molecules such as fullerenes, C_{60} [7,42] and C_{60}^+ [3,8]. Another current area of active research is the investigation of the potential catalytic role of astro-PAHs in the formation of small carbonaceous molecules and H_2 [37,2,5], the most abundant molecule in space. The present paper fits into this general astrophysical context.

Astro-PAHs are admitted to survive most of time in their ground electronic and vibrational states. However, as various sources of energy exist in the ISM, they may receive a large amount of energy, depending on the ISM region. For instance, in molecular clouds, the vicinity of a star creates regions where the photophysics governs the chemical and physical processes. In these regions known as PhotoDissociation Regions (PDRs), a PAH can absorb photons up to 13.6 eV (higher energy photons being absorbed by ubiquitous hydrogen atoms). To investigate PAH photodissociation in such regions, UV-visible photodissociation experiments complemented with static DFT reactions paths' computations and RRKM (Rice-Ramsperger-Kassel-Marcus) unimolecular reaction rate theory modeling to derive rates constants for the most important processes have been achieved [55,57, 56]. This approach allows to treat long timescale events assuming statistical processes and usually with harmonic description of vibrational states. In principle, all isomerisation and dissociation channels should be included in the calculation, which can lead to a very complex mapping of the potential energy surface (PES), as illustrated in the case of the smallest PAH, napththalene [46]. In other environments of the ISM such as the vicinity of a massive star, PAHs may collide with energetic atoms ejected from the star [43,54] while, in shock wave regions, PAHs are exposed to highly energetic collisions [30,29]. To mimic these high energy collisions, experiments, often complemented with molecular dynamics (MD)/force field (FF) simulations, have been achieved (see for instance [17,15,47,48,58,10,23,27, 34]).

Simulating experiments requires the computation on-the-fly of millions of single point energies and gradients to achieve statistically converged simulations. Although this is out of reach with MD/DFT approaches, extensive MD/FF simulations enable the description of long time events. The disadvantage of such ap-

proaches is that reactive force fields such as the AIREBO potential [49,32], are very complex and not always transferable. The lack of description of electronic structure may also result in missing some structures/events while the treatment of charged effects is prevented. Unlike combined DFT/RRKM approaches, no hypothesis on the possible structural evolution is needed and the anharmonic effects of the PES are naturally included. A way to achieve extensive simulations introducing explicitely the electronic structure is to use an approximate DFT-scheme such as Density Functional based Tight Binding (DFTB) approach [33,41,11]. The limitation of such an approach is that simulations can hardly be achieved for more than one nanosecond for a PAH as large as coronene ($C_{24}H_{12}$) for instance [45]. As a result, events occurring at longer timescale are unfortunately ignored.It may be noted that in the case of PAHs for which a variety of isomerisation reactions and dissociation pathways are expected [51,52], even at low energy, MD/DFTB simulations allow to provide insight into reaction mechanisms [35] that can be further probed with more accurate approaches. For instance, MD/DFTB simulations have recently allowed us to probe the dissociation mechanisms and kinetics of the dissociation product of the 1-methylpyrene cation in relation to Infrared multiple photon dissociation (IR-MPD) experiments [22]. Besides, in a similar context as that of the present work, MD/DFTB simulations were carried out to rationalize the effect of the hydrogenation degree on the dissociation pathways of hydrogenated pyrene cations [16].

In this paper, we compare the theoretical and experimental mass spectra resulting from the dissociation of cationic pyrene $C_{16}H_{10}^{+}$ induced by 100 keV protons. The calculated mass spectrum is obtained from extensive MD/DFTB simulations whereas the experimental mass spectrum is measured from high energy particle collision experiments. Although tens of eV are typically deposited in the PAH by proton collision, a rapid and effective internal conversion is assumed, supported by the probable occurence of numerous conical intersections, expected in PAHs[20, 50]. This internal energy is therefore given in the form of vibrational excitation in the PAHs, which remains in its electronic ground-state. Theoretical and experimental approaches are detailed in section 2. The results are reported and discussed in section 3.

2 Methods

2.1 Experimental set up

In this subsection, we briefly describe the experimental set up that allowed us to obtain the experimental spectrum of the pyrene dissociation at high energy, which the theoretical spectrum is compared to.
The SWEET (Stellar Wind and Electron interactions on astrophysical molecules. Experiment and Theory) experiment studies the interactions between particles from stellar winds and isolated molecules that may be present in the circumstellar medium, such as PAHs. The experimental set up includes a pulsed kHz proton accelerator, coupled to a time of flight mass spectrometer (also pulsed) synchronized with the incident protons. The pyrene molecules are produced in their gas phase by a oven heated at around 150 °C. The working pressure is of the order of

10^{-8} Torr. The low molecular density of the jet and the low proton density per pulse (typically a few thousand protons per pulse) guarantee a low probability of interaction for each pulse (less 1 over 1000). The occurence of a ionization event is due to a unique collision between a single isolated molecule and a single proton.

For each event, the mass or masses of the cation(s) produced as the result of the ionization of the pyrene molecule are determined by their flight times. The total mass spectrum of the produced cations is then obtained by summation over all individual events. A more precise description of the experimental setup is given in refs. [9,10]

2.2 Modeling of energy deposit

In this subsection, we describe the model used to determine the amount of deposited energy in the pyrene molecule, which will be used as initial energy distribution for the MD/DFTB simulations. It consists in evaluating the energy lost by the proton and transfered to the target molecule.

Experimentally, for 100 keV protons on pyrene, we respectively observe about 72%, 25%, 3% single, double and triple ionization without fragmentation. The corresponding vertical ionization potentials are 7.43 eV, 18.4 eV, 38.8 eV, the double and triple ionization potentials being evaluated using the MP2 approach in conjunction with a 6-31G basis set. As singly charged species are largely dominant, this study will be devoted to singly charged cations.

The energy lost (E_{ploss}) by the proton is distributed between the ionization potential (IP), the kinetic energy T_{e-} of the emitted electron and the rest is shared to the molecule as 'Excitation energy' E^* via electronic excitation :

$$E_{ploss} = E^* + T_{e-} + IP \tag{1}$$

Rudd et al. [40] have experimentally established that the energy distribution of the emitted electrons from direct ionization in collision process on atomic target follows an exponential decay :

$$P \propto exp(-\alpha E/\sqrt{\epsilon_i T}) \tag{2}$$

with α, a constant depending on the target, E the energy of the emitted electron, ϵ_i the ionization potential of the target, and T the kinetic energy corresponding to an electron having the same velocity as the incident projectile. This empirical law, verified on molecular targets like C_{60} by Rentenier and co-workers [4], indicates that if we consider only non-thermal electronic emission, the most probable kinetic energy carried out by the emitted electron is zero. The average of the distribution for 100 keV incident protons on carbon is around 17 eV (from our measurement of electron spectra emitted during 100 keV proton on pyrene collision (to be published)).
In first approximation, we can therefore consider that the contribution of T_{e-} is relatively low in the energy balance (1) for 100 keV protons on the pyrene. Moreover, given the single ionization potential of 7.43 eV of pyrene (main observed

charge state after interaction), we may infer that a significant part of the energy that can be transferred by the proton to the molecule (depending on the impact parameter of the incident proton and the number of molecular orbitals involved in the interaction) can contribute to 'excitation energy' E^*, leading to the population of an important number of excited electronic states in addition to (mainly) single ionization of the molecule.

The electronic emission from the molecule occurs quickly. Indeed, in the case of collision with 100 keV protons, the longest interaction time is estimated to be τ=16 fs (8 ua) for non-thermal emission [25]. Then the electronic excited state (if not metastable) can quickly relax by fluorescence but also by a rapid internal energy conversion from the electronic to the vibrational states of the molecule. The analysis of PAHs' potential energy surfaces shows canonical intersections [20, 50], which are very efficient for fast redistribution of the energy from electronic to vibrational states, resulting in a heating of the molecule with respect to its number of degree of freedom (if considering equipartition of the energy): $kT = E/(3N-6)$ with N=26 for pyrene. In C_{60}, such heating mechanism accounts for the measured scaling law observed for fragmentation [4]. Mass spectra were found to vary strongly with the collision energy or velocity and the projectile. On the other hand, they scale rather nicely with the energy deposited in the molecule.

In summary, we assume that in first approximation, a large part of the energy loss by the proton is rapidly converted into internal energy resulting in a low degree of ionization of pyrene but with an important internal energy before dissociation. One of the crucial parameters for the study and simulation of pyrene relaxation therefore lies in the amount of internal energy of the molecule after ionization which follows the energy deposited by the projectile in the molecule.

Although it is possible to estimate it [6], the measure of the energy loss of the incident proton is extremely difficult to perform experimentally especially for fast protons (2 ua) since only a small fraction of their kinetic energy is actually transferred (typically a few eV / 100 keV). Direct measurement of this fraction directly will require the use of a very high resolution spectrometer ($\Delta E/E \leq 10^{-6}$)

In order to circumvent these experimental difficulties, we have developed in the LCAR a Monte-Carlo multi-parameter impact code named 'CaspBurn' simulating the energy loss of the proton and thus estimating the energy deposited by the incident projectile. This CaspBurn code is based on the calculation of the energy loss Qe as a function of the impact parameter b of the 100 keV proton incident on the constituent individual atoms of the pyrene molecule (16 C and 10 H), with respect to its geometry and for impact parameters between 0 and 30 Å (see Figure 1).

Atomic $Qe(b)$ extracted from the CASP code [19] and presented in Figure 1 for the diffusion of a 100 keV proton on carbon (red curve) and on hydrogen (black curve) as a function of the impact parameter in Å.

In our experiment, although the collisions are unique and event-by-event, both the relative orientation of the molecule with respect to the incident proton direction and the impact parameter are not known. The orientation of the sublimation-produced molecule has therefore been considered as isotropic and the use of a random selection to simulate the multiple possible orientations of the target molecules

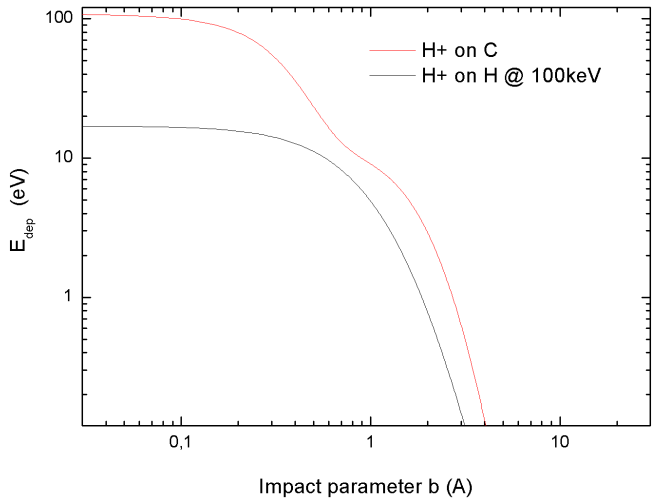

Fig. 1 Energy loss by an incident proton of 100 keV in a carbon and hydrogen atoms

is therefore necessary. Thus our code calculates the classical trajectory of the 100 keV proton through the molecule of pyrene for different orientations of the molecule. These trajectories are considered as rectilinear since at 100 keV, the interaction is mostly electronic is the deviation is negligible. For each trajectory (j) (and orientation), the parameters b_i for the N atoms of the molecule (16C and 10H) are calculated. The total energy Q_j lost by the proton on its trajectory is then deduced by interpolation of the $Q_e(b_i)$ for over all the atoms:

$$Q_j = \sum_{i}^{N} Q_e(b_i) \tag{3}$$

The energy loss distribution by the proton dN/dE during its interaction with pyrene, obtained by averaging over 15 millions of trajectories, is presented in Figure 2 (a) .

As expected, the distribution presents a large number of low energy events corresponding to large impact parameters where there is no (or very little) interaction. The energies used for this low energy part $<$ 2eV are much lower than the ionization threshold of the molecule of 7.43 eV and therefore do not contribute to the experimentally measured fragmentation spectra. There is also a secondary maximum around 20 eV. From this distribution, it is then possible to extract the distribution $P(E_{loss})$ of the energy lost by the proton higher than the threshold of simple ionization of the molecule. This distribution is shown in Figure 2 (b). Considering the assumption made that a large part of the energy deposited by the proton over the ionization threshold contributes to the internal energy of the molecule, this distribution was used as input data for MD/DFTB simulations in

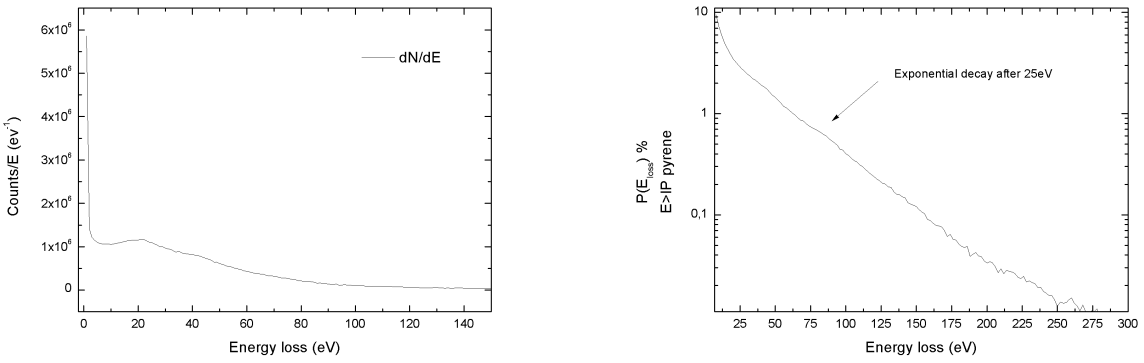

(a) (b)

Fig. 2 (a) Energy loss distribution (a) in counts/eV simulated from the CaspBurn code ; (b) in logarithmic scale, for an energy greater than the pyrene ionization potential

an attempt to reproduce the fragmentation mass spectrum of the pyrene molecule.

2.3 Molecular dynamics simulations

The theoretical mass spectra were determined using the approach described hereafter: several thousands of simulations (up to 4000) of 500 ps each were carried out in the microcanonical ensemble starting from the ground state initial geometry of cationic pyrene. The initial energy of each simulation is randomly withdrawn from the energy distribution obtained as explained in the previous subsection (Fig. 2), after retrieving the ionisation potential of pyrene (taken as 7.43 eV [26]). The simulations at a given energy differ due to the initial random distributions of the kinetic (vibrational) energy over all the atoms of $(C_{16}H_{10})^+$. All simulations are performed within the Born Oppenheimer molecular dynamics model, computing the ground-state potential energy on-the-fly. The nuclei obey the classical equations of motion, integrated with the Verlet's velocity algorithm using a timestep of 0.1 fs.

The purpose of this work is to describe a representative sample of events so as to insure a sufficiently statistical representation of the processes. In this context, the Density Functional based Tight Binding (DFTB) method [33,41,11,13,14,31], which can be regarded as an approximation of DFT with a much lower computational cost while describing explicitly the electronic structure, seems particularly suitable for determining millions of single points and gradients along the trajectories. Regarding the dissociation of cationic PAHs, this approach has been used and benchmarked for a series of model PAHs ranging from naphthalene to coronene [45]. As in [45], we used in this work the second order version of DFTB, also known as Self Consistent Charge (SCC)-DFTB [11], with the mio-set of parameters [11], and the dispersion correction as reported in ref. [36]. We used a Fermi distribution

(Fermi temperature of 1500 K) to determine the molecular orbital occupations in order to avoid oscillation problems when looking for a self consistent solution, often arising when computing SCC-DFTB energy for dissociated or close to dissociation systems.
As only charged fragments are detected in the experiment, for each simulation, at regular time intervals (10 ps (resp. 2 ps) in the case of the 500 ps (resp. 100 ps) simulations), the fragments are analysed and the charge is localised on the largest one, which is the only one kept to undergo subsequent fragmentation. We note that this is an important approximation, all the more requiring a comparison with experimental data to benchmark the approach. Time dependent mass spectra are thus obtained. We may note that the theoretical approach used in the present paper allows us to study only singly ionized species although doubly and thirdly ionized pyrene are formed in the experiments.The results are presented and discussed in Section 3.1.

3 Results

3.1 Theoretical dissociation mass spectra and time evolution

The evolution of the theoretical mass spectra as a function of time are reported in Figure 3. The spectrum of Figure 3 (b) was obtained with a total number of 4000 simulations.One thousand additional simulations of shorter duration (100 ps) were achieved in order to obtain information on the evolution at shorter times, and the resulting spectra are reported in Figure 3 (a).

The evolution of the ratios of the main fragments' and parent ions as a function of time corresponding tho these spectra are reported in Figure 4. Form these figures, one can clearly distinguish two regimes : fast dissociation before $\sim$20 ps involving H-loss in particular, followed by sa lower dissociation regime involving the cleavage of the carbon skeleton. As can be seen in Figure 4 (b) and (d), after 10 ps of simulation time, 37 % of the pyrene cations are fragmented, the yield reaches 42 % after 100 ps , 44 % after 300 ps and finally 45 % after 500 ps. In the following, we describe in details the time evolution of the dissociation spectrum.

As can be clearly seen in Figure 3 (a) and Figure 4 (a), the dehydrogenation channel is the major one at very short times ($<$ 6 ps). After 2 ps, peaks corresponding to m/z equal to 192 up to 201 ie $(C_{16}H_n)^+$ with (n=0-9) are formed with abundances within 2-3 % each with the most abundant dissociation fragments corresponding to single H loss and -2H or -H_2 at 2 ps (see Figure 4 (a)). As time increases, the peak corresponding to H loss (resp. -2H of H_2) decreases up to 1.3 % (resp. 0.8 %) at 10 ps to reach only 0.6 % (resp. 0.3 %) at 100 ps. At longer times (see Figure 3 (b)) , m/z peaks corresponding to m/z=195 (n=3) to 199 (n=7) Da disappear while peaks corresponding to m/z=192-194 (high dehydrogenation degree) and 200-201 (low dehydrogenation degree) remain, however in small abundances. This may indicate that cationic pyrene with intermediate dehydrogenation degrees are more fragile or sufficiently hot to undergo subsequent dissociation with respect $(C_{16}H_9)^+$ or $(C_{16}H_8)^+$, likely to be formed at lower energy and therefore to be colder. In the case of the highest dehydrogenation degrees, all energy must

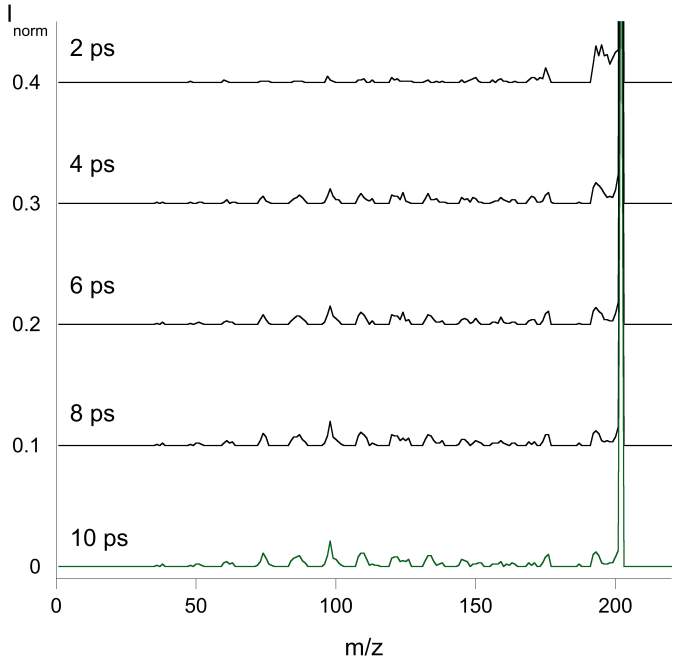

(a)

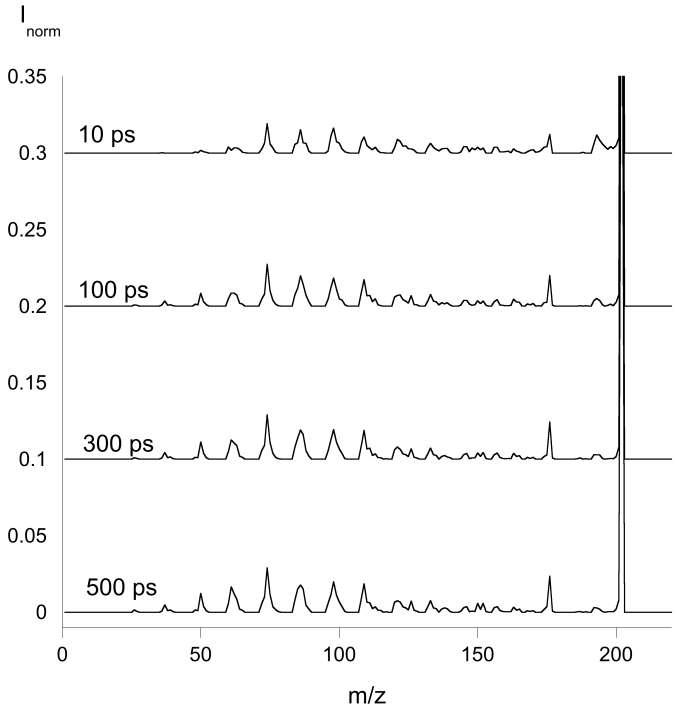

(b)

Fig. 3 Theoretical mass spectra - normalized to the number of trajectories- obtained from MD/DFTB simulations at different times with the energy distribution of Figure 2. The spectra result from the average over (a) 1000 and (b) 4000 simulations.

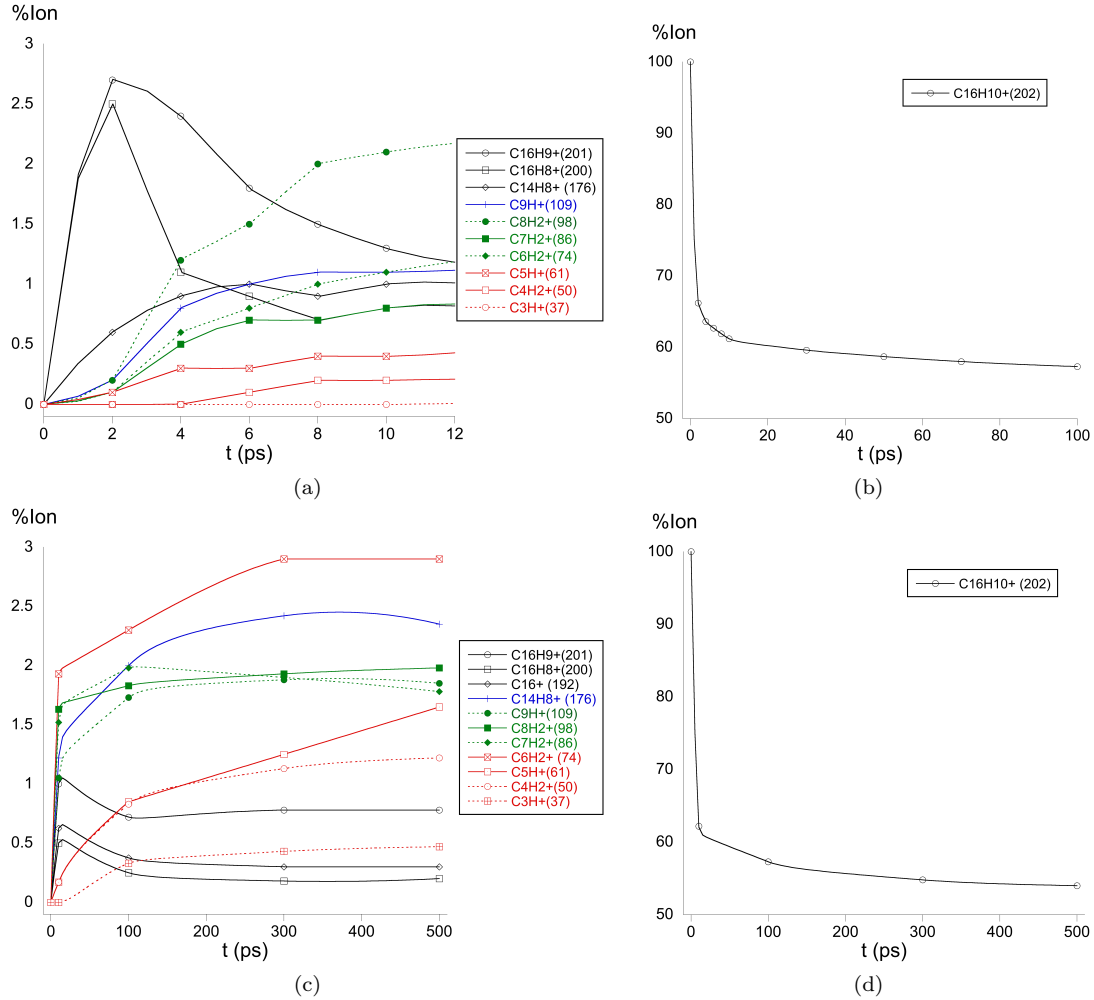

Fig. 4 Evolution as a function of time of the ratio of main fragment (left) and parent (right) ions obtained from extensive MD/DFTB simulations, derived from the mass spectra presented in Figure 3, (a) and (b) : "short times" evolution, 1000 simulations, (c) and (d) : "long times" evolution, 4000 simulations. The m/z values are reminded besides each fragment label. The lines joining the data points are drawn to guide the eyes.

have been taken by the leaving hydrogen atoms (or H_2 molecules). Understanding these behaviors could be the object of future studies.

At short times, the first fragment ion resulting from CC bond cleavage results from the loss of C_2H_2 ($(C_{14}H_8)^+$, see Figure 4 (a)), followed by the formation of $(C_8H_2)^+$, which becomes the most abundant fragment at 12 ps.

At longer times (see Figure 3 (b) and Figure 4 (c)), the most abundant "large mass" fragments ($120 < m/z < 202$) still correspond to $(C_{14}H_8)^+$ (m/z=176 Da, 2 % at 500 ps). Interestingly, no molecular ion fragments resulting from CH_n loss is observed. These results are quite expected as MD/DFTB simulations essentially

describe statistical dissociation processes that are known to lead to H and C_2H_2 loss in the case of PAHs, while loss of CH_n would be due to a non statistical "knock-out" process [17]. Regarding purely dehydrogenated species (with preservation of the C_{16} carbon skeleton), $(C_{16}H_n)^+$ with small values of n (n=0-2), remain with a total ratio of 3 % while singly and doubly dehydrogenated species remain for only 0.8 and 0.2 % respectively. $(C_{16})^+$ also remains in small amounts. A sample of the final geometries of these larger species is reported in Figure 5.When several isomers are considered, the most stable ones are shown in the left column while isomers of higher energy are reported in the right column. Interestingly, when the H/C ratio is small, linear chains are formed whereas when the H/C ratio increases, more compact structures are observed.

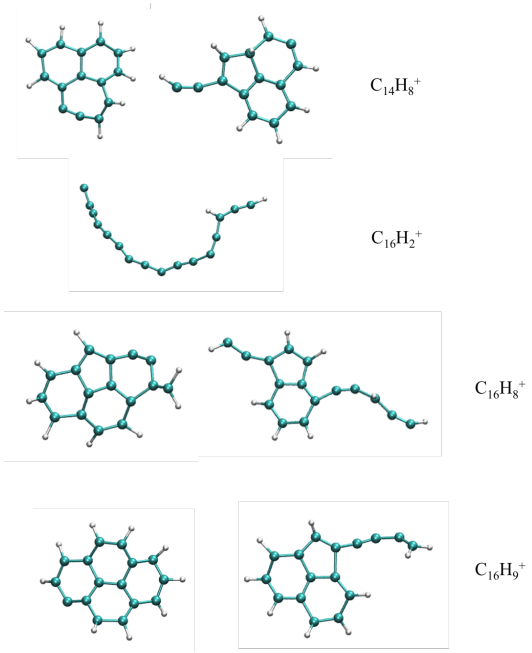

Fig. 5 Sample of of geometries of the largest cationic molecular fragments observed at 500 ps in the MD/DFTB simulations. In case of several isomers, the geometry of the most stable that was found in reported on the left-hand side.

As can be observed in Figure 3 (b), fragments with masses smaller than ∼120 Da are the most abundant after 10 ps. The spectrum becomes quite stable after 100 ps, with however a slight increase of the smallest masses. Among the small masses, the most abundant ones correspond to $(C_6H_n)^+$ (n=0-6), with a maximum for n=2, $(C_6H_2)^+$ (m/z=74 Da), corresponding to 3 % of the total ions at 500 ps (see Figure 4 (c)). As time increases, we note a slight increase of the peak intensity corresponding to the m/z ratio of 60-65 Da, ie $(C_5H_n)^+$ clusters, among which $(C_5H)^+$ is the most abundant and tends to increase at long times (see Figure 4 (b)). At about 2 % ratio are found $(C_7H_{1,2})^+$ (m/z=85-86 Da) ,

$(C_8H_2)^+$ (m/z=98 Da) and $(C_9H)^+$ (m/z=109 Da). Below 2 % ratio are found the smallest molecular ions: $(C_4H_n)^+$ (n=0-4) amongst which the major one is $(C_4H_2)^+$ (m/z=50 Da), and $(C_3H_n)^+$ (n=0-3) (max. $(C_3H)^+$), and finally, the smallest one, $(C_2H_2)^+$ (m/z=26 Da). Insights into the structures of these small fragments are provided in Figure 6. When several isomers have been observed, the most stable ones are reported in the left column while a higher energy one is reported on the right column. As expected for small carbon clusters [53], linear carbon chains are formed.

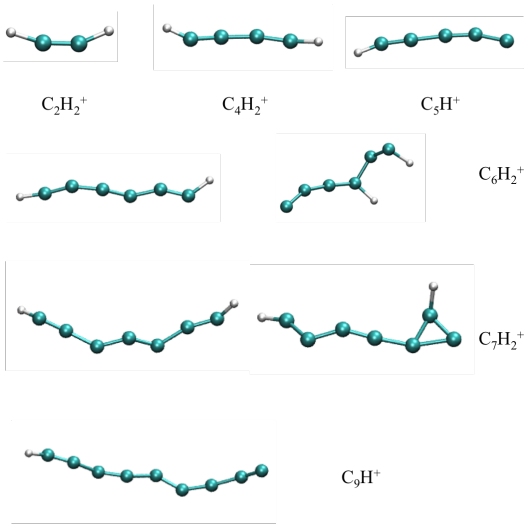

Fig. 6 Sample of geometries of the smallest cationic molecular fragments observed at 500 ps in the MD/DFTB simulations. In case of several isomers, the geometry of the most stable that was found in reported on the left-hand side.

We also determined the distribution of internal energy over all fragments ions at 500 ps by substracting the potential energy of the optimised geometry of the fragment ion to its final total energy at 500 ps. The results are reported in Figure 7. We note a distribution with a maximum a low energy ($\sim$ 2-3 eV), that decreases down to 25 eV, indicating that few dissociation events are expected to be observed in reasonable computational time after 500 ps during the MD/DFTB simulations.

3.2 Theoretical vs experimental mass spectra

As can be seen from Fig. 8, the computed mass spectrum at 500 ps and the experimental one - only focusing on monocationic species- are in relatively good agreement. The comparison between the two spectra leads to the following assertions :
1) The SCC-DFTB potential appears globally gives reliable results for PAHs and

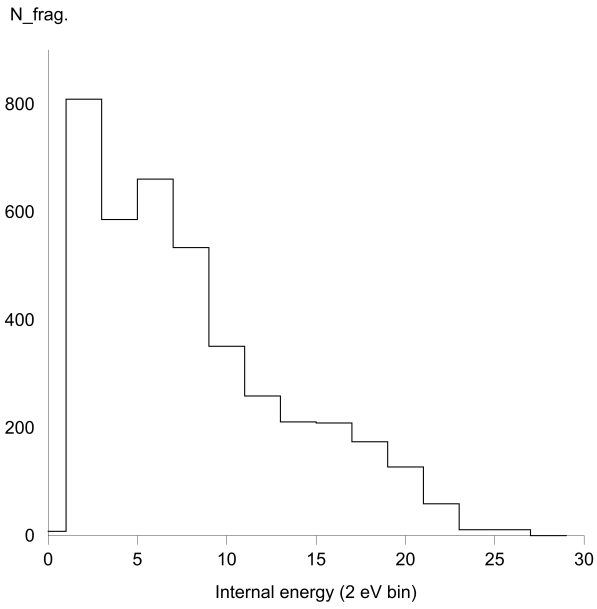

Fig. 7 Distribution of internal energy (in eV, by energy bin of 2 eV) in the fragments ions determined at 500 ps over 4000 MD/DFTB simulations with the initial energy distribution of Figure 2

hydrogenated carbon clusters. However, although the agreement between computed and experimental mass spectra is very good, a difference can be noticed concerning the abundances of dehydrogenated species: the abundance of singly and doubly dehydrogenated pyrene cations in the theoretical spectra seem to be underestimated with respect to the experimental one. This is most likely due to the fact that loss of H is underestimated at low energy in MD/DFTB simulations [45]. It also accounts for the differences in fragmentation yield, which is slightly underestimated in the simulated spectrum with respect to the experimental one.
2) The experimental results are well described with a theoretical description of dissociation in the ground electronic state with internal energy exclusively under the form of vibrational energy (kinetic energy of the nuclei). It seems to validate the general assertion that internal conversion is very effective and that the excited electronic states reached by excitation either by collision or by photon absorption rapidly decay non adiabatically to the ground-state. The non radiative lifetime for PAH radical cations in excited electronic states is indeed expected to be very short (less than several tens of fs [38,39]) because of numerous conical intersections, where non adiabatic decay prevails [20,50]. It also validates the energy distribution model in which this assumption is made. On the whole, thanks to internal conversion, the cations' abundances do not decay by electron emission but rater by dissociation.
3) Most dissociation events occur within a few hundreds of picoseconds, starting from the ionized pyrene.
4) In line with the first point, a wide range of masses are observed and no loss

of "CH_n" is found in the experiment, showing the absence of non statistic dissociation ("knockout" process) that occurs at the lowest energy collision [17,15,47, 48]). This is reproduced by calculations which only describes statistic dissociation events.

We can therefore conclude that dissociation under the present experimental conditions involves statistical processes occurring within few hundreds of piscoseconds, and that these are well reproduced by the MD/DFTB simulations, also allowing to assess the validity of the SCC-DFTB potential.

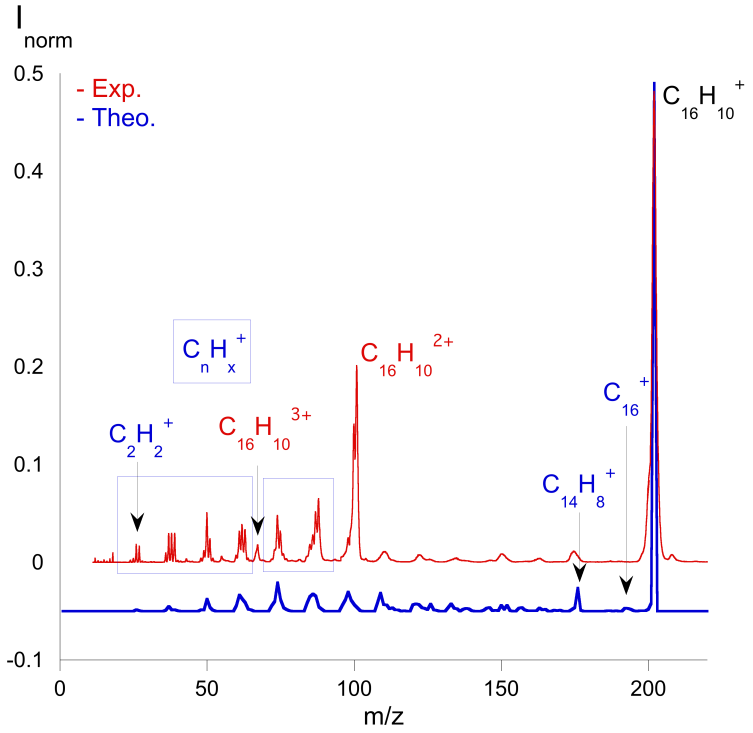

Fig. 8 Experimental mass spectrum (red) obtained after 100 keV H^+ collision with pyrene (see section 2.1) vs theoretical mass spectrum (blue) resulting from 4000 MD/DFTB simulations of 500 ps for cationic pyrene, with the energy distribution of Figure 2 . The experimental spectrum includes all ionisation states while the theoretical ones only includes singly charged species.

3.3 Reconstitution of the distribution of internal energy from theoretical data

In this subsection, we propose to reconstruct the initial energy distribution from the theoretical data in order to validate the atomic model presented in section 2.2.

With respect to the modeling through the Caspburn code (see section 2.2), another way to estimate the internal energy distribution $D(U_i)$ of the cation before dissociation is to reconstruct the mass spectrum obtained experimentally from the theoretical mass spectra $S_{DFTB}(m, U_i)$ at a given initial internal energy U_i. Thus the experimental mass spectrum can be written as:

$$S_{exp}(m) = \int_{U_i=0}^{\infty} D(U_i) S_{DFTB}(m, U_i) dU_i \tag{4}$$

Indeed, starting from the individual DFTB spectra $S_{DFTB}(m, U_i)$, we used a multilinear adjustment to extract the initial internal energy distribution needed to reproduce the experimental mass spectrum. In order to have enough statistics, a binning of the theoretical spectra in steps of δ U=10 eV was performed. The internal energy distribution $D(U_i)$ adjusted on the experimental spectrum (blue histogram) is presented in Figure 9 and compared (in arbitrary unit) to the proton energy loss distribution obtained by our Caspburn code (red curve).

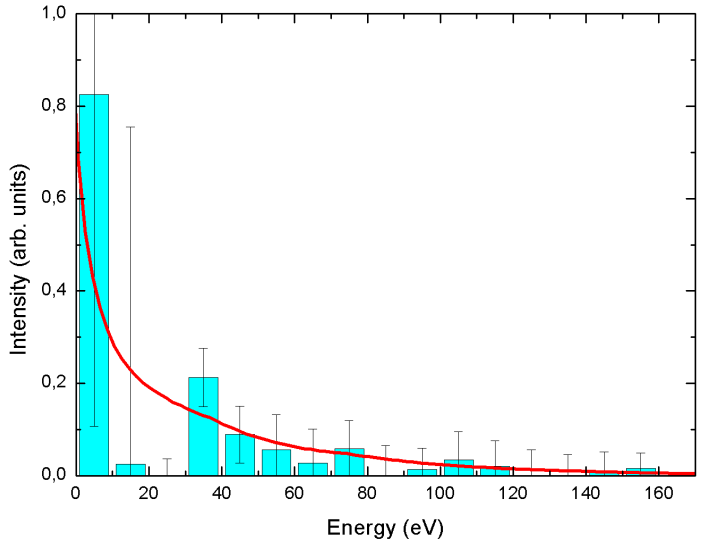

Fig. 9 Energy loss distribution calculated by CaspBurn (red) vs internal energy distribution obtained from experimental mass spectrum fitted with individual DFTB spectra (Blue Rectangle)

Although the statistic of the distribution $D(U_i)$ is a little weak and the associated uncertainties are important, we recover the already discussed exponential trend obtained with Caspburn for proton energy loss distribution P(E) above the ionization threshold. The similarity between the distribution $D(U_i)$ and P(E) reinforces our hypothesis that a significant part of the energy loss by the proton

is effectively (and rapidly) converted into internal energy by the pyrene molecule before it dissociates.

4 Conclusion

Fragmentation of cationic pyrene has been extensively studied by MD/ DFTB simulations using a model to quantify the energy transfered to the target after proton impact, and assuming fast internal conversion for the cations produced. The excitation transfer model is based on atomic contributions while molecular effects are neglected. From this model, after ionisation, the molecules present a wide distribution of internal energy with a rough exponential decrease. This distribution is further used as an input for the MD simulations. Thousands of trajectories are run and the ionic fragments statistics are compared to the experimental mass spectra. A wide range of fragments is produced, with ratios similar to experimental results after 500 ps of simulations, with a majority of small cationic fragments going from $(C_2H_2)^+$ to $(C_9H)^+$. The larger ones result mainly from C_2H_2 loss.

The good agreement between experimental and theoretical spectra globally validates the SCC-DFTB potential, except for dehydrogenation, which is due to the underestimation of H or H_2 loss at low energy in MD/DFTB. The broad distribution of the fragments corresponds to statistical dissociation, with the most abundant remaining cations presumably being the most stable cationic molecules. Second, it validates the scenario both for the deposited internal energy distribution and the fast internal conversion. Finally, adjusting the experimental mass spectrum with the theoretical ones obtained for the various internal energies nicely returns the distribution modeled from the atomic contributions, reinforcing the consistency of the global approach.

Overall, from this study, a scenario emerges for the PAH excited by high energy protons (100 keV): a wide, roughly exponential, distribution of internal energy is deposited in the PAH, produced mainly as monocations. Internal conversion is very fast and effective, relaxation of the vibrational energy excess leads to fragmentation and a wide size of ionic fragments are produced according to statistical dissociation. This study lays the foundations of further synergistic theoretical and experimental studies that will be devoted to other PAHs and prebiotic molecules of astrophysical interest, including the theoretical studies of multicharged species.

5 Acknowledgments

This work is part of the SWEET project (Stellar Wind and Electron interactions on astrophysical molecules. Experiment and Theory), supported through the grant NEXT n^o ANR-10-LABX-0037 in the framework of the "Programme des Investissements d'Avenir". We acknowledge the computing facility CALMIP at the Paul Sabatier University in Toulouse for generous allocation of computer resources. We also thank Georges Trinquier and Pierre Cafarelli for helpful discussions.

References

1. Allamandola, L.J., Tielens, A.G.G.M., Barker, J.R.: Polycyclic aromatic-hydrocarbons and the unidentified infrared-emission bands - auto exhaust along the milky-way. Astrophys. J. **290**(1), L25–L28 (1985).
2. Bentarcurt, Y., Ruette, F., Sánchez, M.: Modeling formation of molecules in the interstellar medium by radical reactions with polycyclic aromatic hydrocarbons. Int. J. Quant. Chem. **110**(13), 2560–2572 (2010).
3. Berné, O., Mulas, G., Joblin, C.: Interstellar C_{60}^{+}. Astron. Astrophys. **550**, L4 (2013).
4. Bordenave-Montesquieu, D., Moretto-Capelle, P., Bordenave-Montesquieu, A., Rentenier, A.: Scaling of C_{60} ionization and fragmentation with the energy deposited in collisions with H^+, H_2^+, H_3^+, and He^+ ions (2-130 keV). J. Phys. B- At. Mol. Opt. Phys. **34**(5), L137–L146 (2001).
5. Boschman, L., Cazaux, S., Spaans, M., Hoekstra, R., Schlathölter, T.: H_2 formation on PAHs in photodissociation regions: a high-temperature pathway to molecular hydrogen. Astron. Astrophys. **579**, A72 (2015).
6. Bredy, R., Bernard, J., Chen, L., Montagne, G., Li, B., Martin, S.: Fragmentation of adenine under energy control. J. Chem. Phys. **130**(11), 114305 (2009).
7. Cami, J., Bernard-Salas, J., Peeters, E., Elizabeth Malek, S.: Detection of c60 and c70 in a young planetary nebula. Science (New York, N.Y.) **329**, 1180–2 (2010).
8. Campbell, E.K., Holz, M., Gerlich, D., Maier, J.P.: Laboratory confirmation of C-60(+) as the carrier of two diffuse interstellar bands. Nature **523**(7560), 322–324 (2015).
9. Champeaux, J.P., Carcabal, P., Rabier, J., Cafarelli, P., Sence, M., Moretto-Capelle, P.: Dehalogenation of 5-halo-uracil molecules induced by 100 keV proton collisions. Phys. Chem. Chem. Phys. **12**(20), 5454–5461 (2010).
10. Champeaux, J.P., Moretto-Capelle, P., Cafarelli, P., Deville, C., Sence, M., Casta, R.: Is the dissociation of coronene in stellar winds a source of molecular hydrogen? application to the hd 44179 nebula. Month. Not. Roy. Astron. Soc. **441**(2), 1479–1487 (2014)
11. Elstner, M., Porezag, D., Jungnickel, G., Elsner, J., Haugk, M., Frauenheim, T., Suhai, S., Seifert, G.: Self-consistent-charge density-functional tight-binding method for simulations of complex materials properties. Phys. Rev. B **58**(11), 7260–7268 (1998).
12. Falvo, C., Friha, H., Pino, T., Dhaouadi, Z., Parneix, P., Calvo, F., Brechignac, P.: Effects of hydrogen dissociation on the infrared emission spectra of naphthalene: theoretical modeling. Phys. Chem. Chem. Phys. **15**, 10241–10250 (2013).
13. Frauenheim, T., Seifert, G., Elsterner, M., Hajnal, Z., Jungnickel, G., Porezag, D., Suhai, S., Scholz, R.: A self-consistent charge density-functional based tight-binding method for predictive materials simulations in physics, chemistry and biology. Phys. Stat. Solidi (b) **217**, 41–62 (2000)
14. Frauenheim, T., Seifert, G., Elstner, M., Niehaus, T., Köhler, C., Amkreutz, M., Sternberg, M., Hajnal, Z., Carlo, A.D., Suhai, S.: Atomistic simulations of complex materials: Ground-state and excited-state properties. J. Phys. Cond. Mat. **14**, 3015 (2002)
15. Gatchell, M., Stockett, M.H., Rousseau, P., Chen, T., Kulyk, K., Schmidt, H.T., Chesnel, J.Y., Domaracka, A., Mery, A., Maclot, S., Adoui, L., Stochkel, K., Hvelplund, P., Wang, Y., Alcami, M., Huber, B.A., Martin, F., Zettergren, H., Cederquist, H.: Non-statistical fragmentation of pahs and fullerenes in collisions with atoms. Int. J. Mass Spectrom. **365**, 260–265 (2014).
16. Gatchell, M., Stockett, M.H., de Ruette, N., Chen, T., Giacomozzi, L., Nascimento, R.F., Wolf, M., Anderson, E.K., Delaunay, R., Vizcaino, V., Rousseau, P., Adoui, L., Huber, B.A., Schmidt, H.T., Zettergren, H., Cederquist, H.: Failure of hydrogenation in protecting polycyclic aromatic hydrocarbons from fragmentation. Phys. Rev. A **92**, 050702 (2015).
17. Gatchell, M., Zettergren, H.: Knockout driven reactions in complex molecules and their clusters. J. Phys. B **49**(16), 162001 (2016).
18. Gillett, F.C., Forrest, W.J., Merrill, K.M.: 8 - 13-micron spectra of NGC 7027, BD +30 3639, and NGC 6572. Astrophys. J. **183**, 87–93 (1973).
19. Grande, P., Schiwietz, G.: Impact-parameter dependence of the electronic energy loss of fast ions. Phys. Rev. A **58**(5), 3796–3801 (1998).
20. Hall, K.F., Boggio-Pasqua, M., Bearpark, M.J., Robb, M.A.: Photostability via sloped conical intersections: Computational study of the excited states of the naphthalene radical cation. J. Phys. Chem. A **110**(50), 13591–13599 (2006).
21. Joblin, C., Tielens, A.G.G.M. (eds.): PAHs and the Universe: A Symposium to Celebrate the 25th Anniversary of the PAH Hypothesis, *EAS Publications Series*, vol. 46 (2011)

22. Jusko, P., Simon, A., Wenzel, G., Brünken, S., Schlemmer, S., Joblin, C.: Identification of the fragment of the 1-methylpyrene cation by mid-ir spectroscopy. Chem. Phys. Lett. **698**, 206 – 210 (2018).
23. Lawicki, A., Holm, A.I.S., Rousseau, P., Capron, M., Maisonny, R., Maclot, S., Seitz, F., Johansson, H.A.B., Rosen, S., Schmidt, H.T., Zettergren, H., Manil, B., Adoui, L., Cederquist, H., Huber, B.A.: Multiple ionization and fragmentation of isolated pyrene and coronene molecules in collision with ions. Phys. Rev. A **83**(2), 022704 (2011).
24. Léger, A., Puget, J.L.: Identification of the 'unidentified' IR emission features of interstellar dust? Astron. Astrophys. **137**, L5–L8 (1984)
25. Lepine, F., Climen, B., Pagliarulo, F., Baguenard, B., Lebeault, M., Bordas, C., Heden, M.: Dynamical aspects of thermionic emission of C-60 studied by 3D imaging. Eur. Phys. J. D **24**(1-3), 393–396 (2003).
26. Lias, S.: "ionization energy evaluation" in the webbook of chemistry NIST number 69 Eds. P.J. Linstrom et W.G. Mallard,National Institute of Standards and Technology, Gaithersburg MD, 20899
27. Martin, S., Chen, L., Bredy, R., Montagne, G., Ortega, C., Schlatholter, T., Reitsma, G., Bernard, J.: Statistical fragmentation of doubly charged anthracene induced by fluorine-beam impact at 3 kev. Phys. Rev. A **85**(5), 052715 (2012).
28. McGuire, B.A., Burkhardt, A.M., Kalenskii, S., Shingledecker, C.N., Remijan, A.J., Herbst, E., McCarthy, M.C.: Detection of the aromatic molecule benzonitrile (c-C6H5CN) in the interstellar medium. Science **359**(6372), 202–205 (2018).
29. Micelotta, E.R., Jones, A.P., Tielens, A.G.G.M.: Polycyclic aromatic hydrocarbon processing in a hot gas. Astron. Astrophys. **510**, A37 (2010)
30. Micelotta, E.R., Jones, A.P., Tielens, A.G.G.M.: Polycyclic aromatic hydrocarbon processing in interstellar shocks. Astron. Astrophys. **510**, A36 (2010)
31. Oliveira, A., Seifert, G., Heine, T., Duarte, H.: Density functional based tight binding : an approximate dft method. J. Braz. Chem. Soc. **20**, 1193–1205 (2009)
32. Parneix, P., Gamboa, A., Falvo, C., Bonnin, M.A., Pino, T., Calvo, F.: Dehydrogenation effects on the stability of aromatic units in polycyclic aromatic hydrocarbons in the interstellar medium: A computational study at finite temperature. Mol. Astrophys. **7**, 9–18 (2017).
33. Porezag, D., Frauenheim, T., Köhler, T., Seifert, G., Kaschner, R.: Construction of tight-binding-like potentials on the basis of density functional theory - application to carbon. Phys. Rev. B **51**, 12947–12957 (1995)
34. Postma, J., Bari, S., Hoekstra, R., Tielens, A.G.G.M., Schlathoelter, T.: Ionization and fragmentation of anthracene upon interaction with kev protons and alpha particles. Astrophys. J. **708**(1), 435–444 (2010).
35. Rapacioli*, M., Simon*, A., Marshall, C.C., Cuny, J., Kokkin, D., Spiegelman, F., Joblin, C.: Cationic methylene-pyrene isomers and isomerization pathways : Finite temperature theoretical studies. J. Phys. Chem. A **119**, 9089–9100 (2015)
36. Rapacioli, M., Spiegelman, F., Talbi, D., Mineva, T., Goursot, A., Heine, T., Seifert, G.: Correction for dispersion and coulombic interactions in molecular clusters with density functional derived methods: Application to polycyclic aromatic hydrocarbon clusters. J. Chem. Phys. **130**(24), 244304–10 (2009)
37. Rauls, E., Hornekær, L.: Catalyzed routes to molecular hydrogen formation and hydrogen addition reactions on neutral polycyclic aromatic hydrocarbons under interstellar conditions. Astrophys. J. **679**(1), 531 (2008)
38. Reddy, S.N., Mahapatra, S.: Theoretical study on molecules of interstellar interest. i. radical cation of noncompact polycyclic aromatic hydrocarbons. J. Phys. Chem. A **117**(36), 8737–8749 (2013).
39. Reddy, S.N., Mahapatra, S.: Theoretical study on molecules of interstellar interest. ii. radical cation of compact polycyclic aromatic hydrocarbons. J. Phys. Chem. B **119**(34), 11391–11402 (2015).
40. Rudd, M.: Ionization by low and intermediate energy ion and neutral beams. IEEE Trans. Nuc. Science **28**(2), 1135–1138 (1981).
41. Seifert, G., Porezag, D., Frauenheim, T.: Calculations of molecules, clusters, and solids with a simplified lcao-dft-lda scheme. Int. J. Quant. Chem. **58**, 185–192 (1996)
42. Sellgren, K., Werner, M.W., Ingalls, J.G., Smith, J.D.T., Carleton, T.M., Joblin, C.: C60 in reflection nebulae. Astrophys. J. Lett. **722**(1), L54 (2010)
43. Siebenmorgen, R., Krügel, E.: The destruction and survival of polycyclic aromatic hydrocarbons in the disks of t tauri stars. A&A **511**, A6 (2010)

44. Simon, A., Rapacioli, M.: Chemical Modelling, *SPR (Specialist Chemical Reports)*, vol. 14, chap. Energetic Processing of PAHs : isomerisation and dissociation, pp. 195–216. Roy. Soc. Chem. (2017)
45. Simon, A., Rapacioli, M., Rouaut, G., Trinquier, G., Gadea, F.X.: Dissociation of polycyclic aromatic hydrocarbons: molecular dynamics studies. Phil. Trans. A **375**, 20160195 (17 pages) (2017)
46. Solano, E.A., Mayer, P.M.: A complete map of the ion chemistry of the naphthalene radical cation? dft and rrkm modeling of a complex potential energy surface. J. Chem. Phys. **143**(10), 104305 (2015).
47. Stockett, M.H., Gatchell, M., Chen, T., de Ruette, N., Giacomozzi, L., Wolf, M., Schmidt, H.T., Zettergren, H., Cederquist, H.: Threshold energies for single-carbon knockout from polycyclic aromatic hydrocarbons. J. Phys. Chem. Lett. **6**(22), 4504–4509 (2015).
48. Stockett, M.H., Zettergren, H., Adoui, L., Alexander, J.D., Berzins, U., Chen, T., Gatchell, M., Haag, N., Huber, B.A., Hvelplund, P., Johansson, A., Johansson, H.A.B., Kulyk, K., Rosen, S., Rousseau, P., Stochkel, K., Schmidt, H.T., Cederquist, H.: Nonstatistical fragmentation of large molecules. Phys. Rev. A **89**(3), 032701 (2014).
49. Stuart, S.J., Tutein, A.B., Harrison, J.A.: A reactive potential for hydrocarbons with intermolecular interactions. J. Chem. Phys. **112**(14), 6472–6486 (2000).
50. Tokmachev, A.M., Boggio-Pasqua, M., Bearpark, M.J., Robb, M.A.: Photostability via sloped conical intersections: A computational study of the pyrene radical cation. J. Phys. Chem. A **112**(43), 10881–10886 (2008).
51. Trinquier, G., Simon, A., Rapacioli, M., Gadéa, F.X.: PAH chemistry at eV internal energy. 1. H-shifted isomers. Mol. Astrophys. **7**, 27–36 (2017)
52. Trinquier, G., Simon, A., Rapacioli, M., Gadéa, F.X.: PaAH chemistry at eV internal energy. 2. Ring alteration and dissociation. Mol. Astrophys. **7**, 37–59 (2017)
53. Van Orden, A., Saykally, R.: Small carbon clusters: Spectroscopy, structure, and energetics. Chem. Rev. **98**(6), 2313–2357 (1998).
54. Visser, R., Geers, V.C., Dullemond, C.P., Augereau, J.C., Pontoppidan, K.M., van Dishoeck, E.F.: Pah chemistry and ir emission from circumstellar disks. A&A **466**(1), 229–241 (2007)
55. West, B., Joblin, C., Blanchet, V., Bodi, A., Sztaray, B., Mayer, P.M.: On the dissociation of the naphthalene radical cation: New ipepico and tandem mass spectrometry results. J. Phys. Chem. A **116**(45), 10999–11007 (2012).
56. West, B., Sit, A., Mohamed, S., Joblin, C., Blanchet, V., Bodi, A., Mayer, P.M.: Dissociation of the anthracene radical cation: A comparative look at ipepico and collision-induced dissociation mass spectrometry results. J. Phys. Chem. A **118**(42), 9870–9878 (2014).
57. West, B., Useli-Bacchitta, F., Sabbah, H., Blanchet, V., Bodi, A., Mayer, P.M., Joblin, C.: Photodissociation of pyrene cations: Structure and energetics from $c_{16}h_{10}^{+}$ to c_{14}^{+} and almost everything in between. J. Phys. Chem. A **118**(36), 7824–7831 (2014).
58. Zhen, J., Castellanos, R., Paardekooper, D.M., Ligterink, N., Linnartz, H., Nahon, L., Joblin, C., Tielens, A.G.G.M.: Laboratory photo-chemistry of pahs: ionization versus fragmentation. Astrophys. J. Lett. **804**(1), L7 (2015).